

Production of ZnO and Zn–ZnO Nanopowders Using Evaporation by a Pulsed Electron Beam and Condensation in a Low-Pressure Gas

V.G. Il'ves, Yu.A. Kotov, and S.Yu. Sokovnin

*Institute of Electrophysics Ural Branch RAS, 106, Amundsen str., Ekaterinburg, 620216, Russia
E-mail: sokovnin@iep.uran.ru*

Abstract – A method for making of ZnO and Zn–ZnO nanopowders using evaporation of a target by a pulsed electron beam and condensation in a low-pressure gas on a cold crystallizer is developed.

Crystalline and amorphous nanopowders of pure ZnO and a Zn–ZnO mixture were produced. The powders have the specific surface of up to 40 m²/g at the output capacity of up to 5 g/h.

It is found that the pressure and the composition of the gas (air, oxygen, argon) in the evaporation chamber of the installation influence the mixture and the morphology of the nanopowders.

The effect of the target composition on the characteristics of the powders and the output capacity is analyzed. All the powders have magnetic characteristics.

1. Introduction

ZnO is a direct gap semiconductor with the forbidden gap 3.37 eV wide and a high binding energy of the exciton equal to 60 meV. This material possesses unique piezoelectric, optical, sensor and magnetic properties, which make it promising for use in nanoelectronics, optoelectronics, spintronics, ultraviolet and blue lasers, etc. [1, 2].

The known physical methods of vapor deposition, which are used for synthesis of ZnO nanostructures, include widely popular techniques of thermal heating with or without catalysts, pulsed laser deposition and magnetron sputtering [3].

Therefore, it is reasonable to check if the method of evaporation by a pulsed electron beam in a low-pressure gas [4] is applicable to production of nanopowders of ZnO.

The main objective of the work was to produce a monodispersed ZnO powder and subsequent analysis of its properties so as to determine possible applications of this material.

2. Experimental technique

The experiments were performed on a modernized “Nanobeam-2” installation, which had, as compared to its prototype [4], a more powerful electron gun and another design of the crystallizer (a hollow cylinder 300 mm in diameter and 500 mm long).

The parameters of the installation and methods of analysis of the synthesized materials was the same as in [5].

The tasks of the experiments were to determine the optimal composition of both the target and the evaporation medium for synthesis of a pure material. Also, a significant point was determination of the maximum possible capacity of the method.

Considering the availability of materials for making of the target (compaction in a hand press), the following materials were used:

- a ZnO powder (chemically pure, GOST 10262-73) containing one ZnO phase with the coherent scattering region (CSR) equal to ≈ 200 nm and the lattice spacings: $a = 3.251$ Å and $c = 5.209$ Å;

- a ZnO nanopowder (nano) with the specific surface of about 10 m²/g, which was synthesized by the EEW method [9];

- a ZnO nanopowder (mix) representing a mixture of ZnO (chemically pure) and ZnO (nano) oxides in the mass ratio of 9:1, 7.1:3, and 1:1, respectively;

- cast metal targets made of granulated Zn of the grade (GOST 6-09-5294-86).

The powdered targets had the diameter of 40 to 60 mm and the height of 10 to 20 mm. The cast targets were 40 mm in diameter and about 10 mm high. To decrease the heat loss, the cast targets were placed on a cushion of a micron-sized YSZ powder (which was chosen for its high melting point and inertness) 5 mm thick.

The targets were evaporated in the atmosphere of technical oxygen (GOST 5583-78), technical argon (GOST 10157-70) and mixtures of these gases in different ratios.

3. Experimental results

The obtained results were given in Table 1.

The cheapest starting material was ZnO (chemically pure) and, for this reason, the possibility of using it as the material of the target was checked. Table 1 (Nos. 6 to 14) gives experimental results concerning the evaporation of ZnO (chemically pure) targets at different oxygen pressures in the evaporation chamber of the “Nanobeam-2” installation.

The obtained results suggested that the specific surface S_s was not over 29 m²/g at the output capacity of about 1 g/h, while the pressure dependence of S_s was nonlinear and had a marked maximum near $P_{O_2} = 20$ Pa. As P_{O_2} increased to 50 Pa, the powder yield dropped and S_s increased. As the oxygen pressure increased, the color of the powders changed from black-gray to white, pointing to the presence of zinc in the powders evaporated at pressures less than 50 Pa.

Table 1. Results of experiments on the evaporation of ZnO targets

Ord. No.	Gas pressure, Pa	S_s , m ² /g	Frequency, Hz	Target material	Gas	Beam scanning area, cm ²	$M_{collect}$, g/h
1	20	28.7	100	ZnOnano	Argon	1.5	2.4
2	35	35.1	100	ZnOnano	Argon	1.5	0.9
3	40	30	100	ZnOnano	Argon	1.5	0.6
4	20	36.9	50	ZnOnano	Argon	4.0	0.6
5**	30	38.5	100	ZnO ch.pure	Argon	4.0	0.2
6	16	5.3	100	ZnO ch.pure	Oxygen	1.5	1.05
7	20	13.2	50	ZnO ch.pure	Oxygen	4.0	0.12
8	20	29.1	100	ZnO ch.pure	Oxygen	1.5	1.6
9	28	7	100	ZnO ch.pure	Oxygen	1.5	0.8
10	45	17	100	ZnO ch.pure	Oxygen	4.0	1.2
11	45	24.4	50	ZnO ch.pure	Oxygen	4.0	0.2
12	50	17.8	50	ZnO ch.pure	Oxygen	1.5	0.2
13	50	19.3	100	ZnO ch.pure	Oxygen	1.5	0.6
14	16–35	26.9	50–100	ZnO ch.pure	Oxygen	1.5	No data
15	20	17.5	100	ZnOmix (1:1)	Oxygen	1.5	0.6
16	35	9.62	100	ZnOmix (7:3)	Oxygen	1.5	0.4
17	20	23.3	100	ZnOmix (9:1)	Oxygen	1.5	0.36
18	22	24.4	50	Zn	Oxygen	1.5	1.95
19	22	70.7	50	Zn	Oxygen	0.15	0.15
20	50	35	50	Zn	Oxygen	0.15	0.51
21	3,8	35.7	50	ZnOnano	Vacuum	0.15	4.0
22	5	56.6	50	ZnOnano	Vacuum	4.0	2.4
23	45	40	50	ZnO ch.pure	Air	4.0	0.2
24	20	38	50	ZnO ch.pure	Air	4.0	No data

Note. * The samples were taken from the external wall of the crystallizer. ** A warm crystallizer.

According to the RDA data, the samples evaporated at a pressure of 50 Pa (Table 1, No. 12) were practically pure zinc oxide. It follows from the image obtained in a scanning microscope (Fig. 1) that the agglomerated powders synthesized at an oxygen pressure of 50 Pa consisted of crystalline nanostructures up to 150 nm in size having clear-cut faceting.

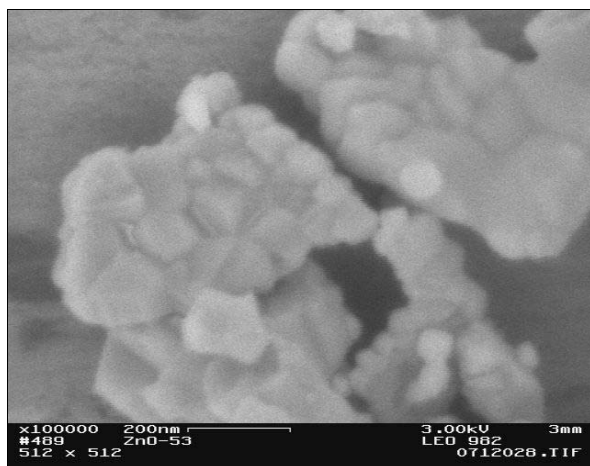


Fig. 1. SEM of the nanopowder (Table 1, No. 6)

The obtained results were showed that average beam intensity on the target surface in the evaporation zone has considerable action upon S_s .

As the average beam intensity on the target surface in the evaporation zone decreased, because of the scanning area of the beam on the target was increased from 1.5 till 4 cm² (Table 1, Nos. 11 and 12), the specific surface S_s increased from 17.8 till 24.4 m²/g. The same effect was confirmed when the pulse repetition rate (so average beam intensity) was increased from 50 till 100 pps (Table 1, Nos. 10 and 11), the specific surface S_s decreased to 17 m²/g, but the output capacity was six times more.

To increase the output capacity, with the view of using the catalytic mechanism of ZnO evaporation in zinc vapor, we studied a ZnO (nano) powder as the material of the target. An inert atmosphere was used.

Table 1 (Nos. 1 to 6) gives experimental results obtained at different argon pressures in the evaporation chamber of the installation. It follows from these results that the specific surface S_s was not over 37 m²/g at the output capacity of about 2.5 g/h, while the pressure dependence of S_s exhibited a nonlinear behavior with a marked maximum near $P_{O_2} = 35$ Pa.

The powders had a black color in all the experiments. The powders grew lighter upon heating during the BET analysis. One of the samples caught fire on its exposure to air, indicating a high concentration of zinc in the powders synthesized by evaporation of ZnO (nano) targets in argon, i.e., oxidation of free zinc took place.

Unfortunately, the ZnO (nano) powder cannot always be used as the material of the targets because it is expensive and scarce. Therefore, the possibility of decreasing its proportion in the targets was studied. Targets made of a ZnO (mix) powder (Table 1, Nos. 15 to 17) were evaporated in an oxygen atmosphere for synthesis of pure ZnO. The mass of the evaporated material of the target increased with growing percentage of ZnO (nano); as the oxygen pressure increased, the yield of the powder from the crystallizer diminished.

It should be noted that edges of the crater, which was formed during the evaporation of the targets made of the ZnO (mix) and ZnO (chemically pure) powders, were considerably different from those formed during the evaporation of ZnO (nano) targets. The crater edges on the ZnO (mix) and ZnO (chemically pure) targets were uneven and had a dendrite structure. The crater on the targets made of the ZnO (nano) powder was round and had smooth edges irrespective of the gas composition in the evaporation chamber.

The green color of the crater walls (about 1–2 mm thick) suggested a considerable concentration of zinc and the catalytic mechanism of the ZnO evaporation in zinc vapor. The green color on the imprint edges appeared also on the ZnO (mix) target with a large concentration (1:1) of the nanopowder.

The obtained data demonstrated that the target composition is essential at the evaporation stage. A considerable effect was due also to the gas composition and the average beam intensity of the target surface. Therefore, it stands to reason to evaporate metals having a lower melting point.

The evaporation of cast zinc targets in oxygen demonstrated (Table 1, Nos. 18 to 20) that the mass of the evaporated material of the target was up to 31.5 g/h ($S_s = 24.4 \text{ m}^2/\text{g}$). Thus, the metal was evaporated very efficiently.

The main drawback of the evaporation of targets made of pure Zn is the impossibility of turning the target toward the crystallizer (because of the formation of a liquid bath) and this strongly affects the amount of the powder collected from the crystallizer.

Also, thermal insulation of the target from the substrate has a considerable effect on the evaporation mechanism. If thermal insulation is good (the target is sunk in the bath in the YSZ pellet), zinc is boiling with ejection of droplets; if thermal insulation is unsatisfactory (the layer of the YSZ powder is thin), the evaporation of the target is weak.

Targets were evaporated in a vacuum at a residual pressure of 3.8–5 Pa so as to decrease the beam loss

through the scattering by the gas atoms. Two targets were evaporated (Table 1, Nos. 21 and 22). The specific surface of the samples was 35–56 m^2/g and the powder output was increased.

The sample No. 22 was evaporated to an uncooled copper crystallizer at a maximum sweep of the beam (4 cm^2) and the sample No. 21 was evaporated to a cooled wall of a stainless steel crystallizer at the sweep of 1.5 cm^2 .

Different values of S_s for the samples Nos. 21 and 22 suggested that the average beam intensity on the surface of the evaporated target had a greater effect on the specific surface.

It follows from the microscopic analysis of the sample No. 22 that the evaporation in a vacuum provided different ZnO and Zn–ZnO nanostructures (according to the RDA data, the sample No. 22 had the following composition: 39% Zn (CSR = 39 nm), 5% ZnO (CSR > 200 nm), and 56% ZnO (CSR = 3 nm), which were faceted well. It is seen (Fig. 2) that as the size of the synthesized particles changed, the transition from particles having the size of units of nm (probably amorphous) to faceted (hexagonal, columnar and another geometrical shape) structures 10 to 200 nm in size took place.

It should be noted that hexagonal ZnO nanostructures (textured Zn–ZnO nanodisks), which are very much like our hexagonal structures, were purposefully obtained by the carbothermal synthesis in [6]. ZnO nanodisks, which were made in [6], had a large size (100–200 nm thick and up to 5 μm wide). In other words, separate regularly shaped particles less than 100 nm in size, as in our case, were obtained for the first time.

The powders, which were synthesized in a vacuum, had a black color because of a large concentration of zinc, which was initially present in the target material and increased additionally due to the decomposition of ZnO on account of a high evaporation temperature.

The samples Nos. 23 and 24 were evaporated under the same conditions, but the condensation conditions were different. The powder from the sample No. 24, which was deposited on the uncooled copper crystallizer at $P_{\text{air}} = 20 \text{ Pa}$, had a black color and reacted with the copper wall of the crystallizer.

According to the RDA data, the synthesized powder contained a large concentration of impurity copper in the nanoform and zinc [15% Zn (CSR = 10 nm), 4% ZnO (CSR > 200 nm), 70% ZnO (CSR = 3 nm), and 11% Cu (CSR = 32)].

The sample No. 23 and the powder were deposited on the stainless-steel walls of the evaporation chamber. The synthesized powder had a black color and $S_s = 40 \text{ m}^2/\text{g}$. The sample also contained zinc [23% Zn (CSR = 6 nm), 12% ZnO (CSR > 200 nm), and 65% ZnO (CSR = 3.8 nm)] and a weak line of an impurity (most probably, iron) was observed.

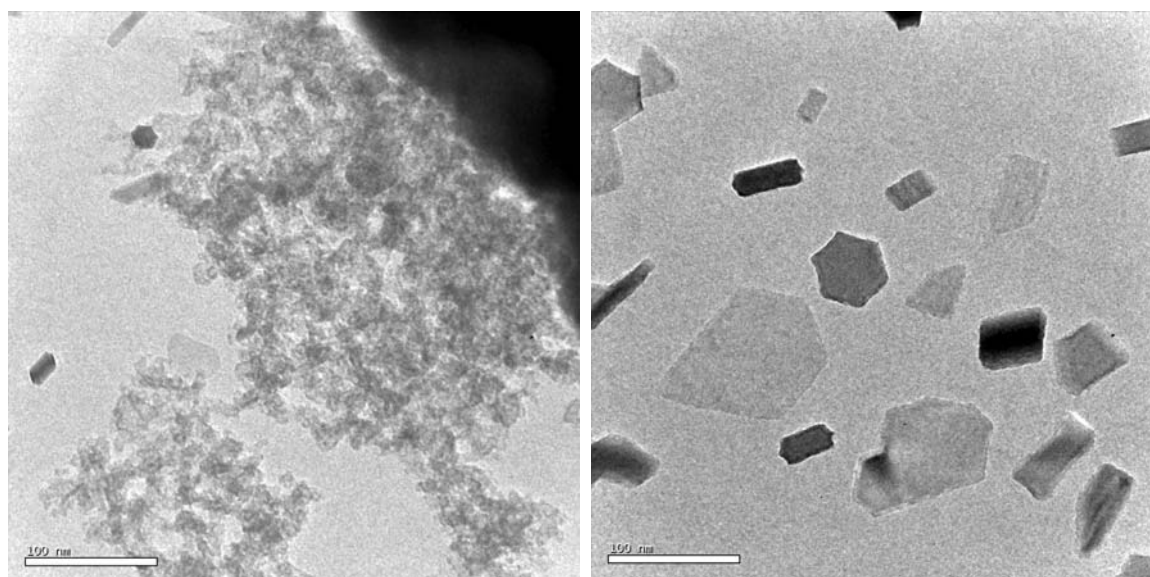


Fig. 2. ZnO nanostructures synthesized by the electron beam evaporation in a vacuum

Thus, ZnO nanopowders with large S_s can be produced by evaporation in air, but the zinc concentration remains at a level of 20%. Moreover, the powder yield was small when ZnO (chemically pure) targets were evaporated.

Additional experiments were performed with the aim of increasing the proportion of the powder collected on the crystallizer – the efficiency – by increasing the distance between the deflecting coil edge and the target from 80 to 170 mm. The analysis of the obtained results shows that as the distance from the deflecting coil edge to the target increases, the mass of the evaporated material decreases, but the efficiency is improved considerably, especially when the target is tilted toward the crystallizer.

All the samples had magnetic properties.

4. Conclusions

Our experiments allow determining the main factors that have effect on the output capacity of the installation and properties of the ZnO powders. The obtained results show that.

1. The proposed method allows making agglomerates of the ZnO powders with S_s up to $40 \text{ m}^2/\text{g}$ at the output capacity up to 5 g/h and faceted nonagglomerated powders 20–100 nm.

2. The target composition has a considerable effect on the yield and properties of the powder; this especially applies to impurity zinc, even in small quantities.

3. A significant point is not only the electron beam energy of a pulse, but also the distribution of this energy on the target surface with time. As the average

beam intensity is reduced, S_s grows, but the output capacity decreases.

4. The composition of the atmosphere used for evaporation of the target influences not only the chemical composition of the synthesized powders, but also the size of their particles. As the oxygen concentration increases, the specific surface diminishes, but pure ZnO is synthesized.

Acknowledgements

The authors wish to thank T.M. Demina, who measured the specific surface of the powders, A.M. Murzakayev for the electron microscopic examination of the samples, A.I. Medvedev, who performed the X-ray diffraction analysis, A.V. Bagazeyev for the EEW powders.

References

- [1] U. Ozgur, Ya.I. Alivov, C. Liu et al., *J. Appl. Phys.* **98**, 041301–103 (2005).
- [2] Z.L. Wang, *J. Phys. Condens. Matter* **16**, 829 (2004).
- [3] A.I. Guzev, *Nanomaterials, Nanostructures and Nanotechnologies*, Moscow, Fizmatlit, p. 416.
- [4] V.G. Ilves, Ya.A. Kotov, S.Yu. Sokovnin, and C.K. Rhee, *Rossijskie Nanotekhnologii* **2**, 96 (2007).
- [5] G.V. Il'ves, A.S. Kamenetskikh, Yu.A. Kotov et al., *in 9th Inter. Conf. on Modification of Materials with Particle Beams and Plasma Flows*, Tomsk, Russia, 2008.
- [6] Z. Fan and J.G. Lu, *Nanoscience and Nanotechnology* **5**, 1561 (2005).
- [7] Yu.A. Kotov, *J. of Nanoparticle Res.* **5**, 539 (2003).